PERGAMON

International Journal of Heat and Mass Transfer 45 (2002) 2567–2575

International Journal of HEAT and MASS TRANSFER

www.elsevier.com/locate/ijhmt

A numerical model for the mixing of an inclined submerged heated plane water jet in calm fluid

P.B. Angelidis *

School of Engineering, Democritus University of Thrace, Xanthi 67100, Greece

Received 30 October 1999; received in revised form 19 October 2001

Abstract

The basic objective of this paper is the presentation of a numerical model for the mixing of an inclined submerged heated plane water jet in calm fluid, which has some improvements over similar models presented by various other investigators. The basic features of our model are: the conservation of heat flux instead of conservation of the buoyancy flux, the inclusion of the turbulent heat flux integrated across the jet, and the modification to include entrainment coefficient depending on the local Richardson number. This model predicts with reasonable accuracy experimental results regarding the axial dilution and the trajectory.

1. Introduction

An inclined submerged heated water jet is produced by the discharge of heated effluents through a diffuser with ports at an angle with the vertical. The mechanics of buoyant jet flows are presented by List [1,2]. Various numerical models have been proposed to study this problem, see for example, Fan and Brooks [3], Anwar [4], Chan and Kennedy [5], Lee [6]. In the previous numerical models, the contribution of the turbulent heat flux integrated across the jet was neglected. Also the use of constant entrainment coefficient did not help to an accurate simulation of these kinds of flows. The improvements of this model are to use the conservation of heat flux instead of buoyancy flux, which is more suitable for cooling water plume dilution models, to include the contribution of the turbulent heat flux and to use an entrainment function that varies with Richardson number.

2. Description of the numerical model

The mathematical model of the problem is given by the following equations in an appropriate coordinate system indicated in Fig. 1.

Variables s and n are the natural (curvilinear) coordinates. Variable s measures the distance along the jet axis from the origin and n is the coordinate perpendicular to the jet axis; overbar indicates time mean values and prime turbulent fluctuations; ρ_a is the ambient density; $\overline{P}$ is the (mean) pressure, $\overline{T}$ is the mean excess temperature; u and v are, respectively, the velocities along the s and n axis. Assuming Boussinesq approximation we may write:

Conservation of mass:

$$\frac{\partial \overline{u}}{\partial s}+\frac{\partial \overline{v}}{\partial n}=0. \tag{1}$$

Conservation of momentum:

- s-momentum

$$\overline{u}\frac{\partial \overline{u}}{\partial s}+\overline{v}\frac{\partial \overline{u}}{\partial n}=-\frac{1}{\rho_a}\frac{\partial \overline{P}}{\partial s}-\frac{\overline{\rho}-\rho_a}{\rho_a}g\sin\theta-\frac{\partial \overline{u'^2}}{\partial s}-\frac{\partial \overline{u'v'}}{\partial n}. \tag{2}$$

- n-momentum

$$\overline{u}\frac{\partial \overline{v}}{\partial s}+\overline{v}\frac{\partial \overline{v}}{\partial n}=-\frac{1}{\rho_a}\frac{\partial \overline{P}}{\partial n}-\frac{\overline{\rho}-\rho_a}{\rho_a}g\cos\theta-\frac{\partial \overline{u'v'}}{\partial s}-\frac{\partial \overline{v'^2}}{\partial n}. \tag{3}$$

Conservation of heat:

$$\overline{u}\frac{\partial \overline{T}}{\partial s}+\overline{v}\frac{\partial \overline{T}}{\partial n}=-\frac{\partial \overline{u'T'}}{\partial s}-\frac{\partial \overline{v'T'}}{\partial n}. \tag{4}$$

* Present address: 2 Parthenonos Street, 67100 Xanthi, Greece.

E-mail address: pangelid@xan.forthnet.gr (P.B. Angelidis).

0017-9310/02/$ - see front matter
PII: S0017-9310(01)00341-6

Nomenclature

List of symbols

$b_{1/eT}$	value of n at which the mean temperature takes the value $\overline{T}_m/e$
$b_{1/eu}$	value of n at which the mean velocity takes the value $\overline{u}_m/e$
b_u	value of n at which the mean velocity takes the value $\overline{u}_m/2$
D	width of the plane jet at the exit
F_L	local Froude number
g	acceleration of gravity
H_0	input heat flux
H_M	heat transport by the mean flow
H_T	turbulent heat flux
$m(s)$	local momentum flux
n	coordinate perpendicular to the jet axis
$\overline{P}$	mean pressure
R_{ch}	Richardson number
s	distance along the jet axis from the origin
$\overline{T}$	mean excess temperature
T_a	temperature of the ambient fluid
$\overline{T}_m$	temperature at the jet axis
T_0	temperature of the heated plane water jet at the exit
u	velocity along the s axis
$\overline{u}_m$	axial velocity at distance s
U_0	initial velocity at the jet axis
v	velocity along the n axis
$\overline{v}_e$	entrainment velocity
α_e	entrainment coefficient

Greek symbols

$\beta(s)$	local buoyancy flux
θ	angle of inclination
λ	the ratio $b_{1/eT}/b_{1/eu}$
$\mu(s)$	local mass flux
ρ	density
ρ_a	density of the ambient fluid
$\overline{\rho}_m$	density at the jet axis
ρ_0	density of the heated plane water jet at the exit

The above equations can be integrated across the buoyant jet to obtain the following integral equations:

Conservation of mass:

$$\frac{d}{ds}\int_{jet}\overline{u}(s,n)\,dn = -2\overline{v}_e = 2\alpha_e\overline{u}_m, \tag{5}$$

where $\overline{v}_e$ is the entrainment velocity, α_e the entrainment coefficient and $\overline{u}_m$ is the axial velocity at distance s.

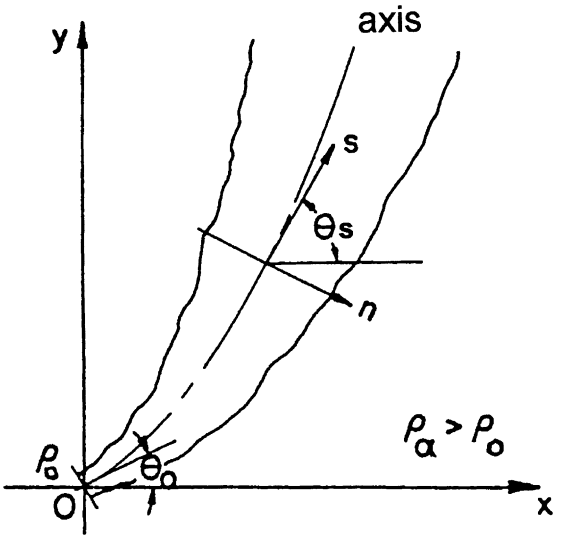

Fig. 1. Geometry of an inclined submerged heated plane water jet.

Conservation of momentum:

- s-momentum

$$\int_{jet}\left(\overline{u}\frac{\partial\overline{u}}{\partial s}+\frac{\partial\overline{u'}^2}{\partial s}+\frac{1}{\rho_a}\frac{\partial\overline{P}}{\partial s}\right)dn = \int_{jet}\left(\frac{\rho_a-\overline{\rho}}{\rho_a}g\sin\theta\right)dn. \tag{6}$$

- n-momentum

$$\int_{jet}\left(\overline{u}\frac{\partial\overline{v}}{\partial s}+\frac{\partial\overline{u'v'}}{\partial s}+\frac{\partial\overline{v'}^2}{\partial n}+\frac{1}{\rho_a}\frac{\partial\overline{P}}{\partial n}\right)dn = \int_{jet}\left(\frac{\rho_a-\overline{\rho}}{\rho_a}g\cos\theta\right)dn. \tag{7}$$

Conservation of heat:

$$\int_{jet}\left(\overline{u}\frac{\partial\overline{T}}{\partial s}+\frac{\partial\overline{u'T'}}{\partial s}\right)dn = \int_{jet}\overline{u}\overline{T}\,dn+\int_{jet}\overline{u'T'}\,dn = H_M+H_T = 0 \quad \text{or} \tag{8}$$

$$\int_{jet}(\overline{u}\overline{T}+\overline{u'T'})\,dn = H_0 = \text{input heat flux}, \tag{9}$$

where H_0 is the input heat flux, $H_M=\int_{jet}\overline{u}\overline{T}\,dn$ is the cross-sectional heat transport by the mean flow and $H_T=\int_{jet}\overline{u'T'}\,dn$ is the cross-sectional heat transport by the turbulence.

The resulting numerical model is an integral model of the flow of the type that Fan and Brooks [3] used to study numerically the behavior of buoyant jets.

However, our model has some improvements. The basic new features of this model are the following:

2.1. The inclusion of turbulent heat flux in the equation of conservation of heat

All the previous models (i.e. Fan and Brooks [3], Chan and Kennedy [5], Hirst [7], Lee [6]) assumed that the integral across the jet of the turbulent heat (and consequently buoyancy) flux can be neglected. However, the contribution of the turbulent heat flux H_T integrated across the jet is not negligible, and according to Kotsovinos [8], Kotsovinos and List [9] the turbulent heat flux H_T reach 30–40% of the total heat flux H_0 for a vertical plane plume. This feature of the flow is very important and should be included in the integral type numerical models. The ratio of the turbulent transfer of heat H_T to the total heat transfer H_0 is a function of the local importance of buoyancy forces which are expressed by the local Richardson number

$$R_{ch} = \frac{\mu^3 \beta}{m^3}, \tag{10}$$

where $\mu(s)$, $\beta(s)$ and $m(s)$ are the local values of the fluxes of mass, buoyancy and momentum across the jet. The Richardson number is the reciprocal of the local Froude number F_L i.e.

$$R_{ch} = \sqrt{\frac{8\pi\lambda^2}{\ln 2(1+\lambda^2)}} \frac{1}{F_L^2}. \tag{11}$$

For a pure plane jet $R_{ch} = 0$ and for a pure plane plume $R_{ch} = 0.6$. In this numerical model, a relationship between the turbulent heat flux H_T and the H_0 similar to the one proposed by Kotsovinos and List [9] was adopted.

$$H_T(s) = (0.06 + 0.51 R_{ch}(s)) H_0. \tag{12}$$

The experimental coefficients in the above equation are suggested from the experimental results of the experimental data of Angelidis [10].

2.2. The conservation of the heat flux (and not the buoyancy flux)

Fan and Brooks [3] as well as most previous investigators adopted the basic conservation approach of Morton et al. [11] and they assume the conservation of density deficiency which implies that buoyancy flux of a buoyant jet in a homogeneous ambient fluid is conserved. This assumption was adopted by most previous investigators considering it accurate and they applied this assumption in buoyant water jets independently of the origin of the buoyancy, i.e. salt or heat. The assumption of conservation of the buoyancy flux is not accurate for thermal water jets. Lemieux [12] conducted experiments with horizontal plane thermal jets and noticed that the experimentally determined trajectories do not agree with the prediction of a numerical model similar to the models of Fan and Brooks [3] or the model of Chan and Kennedy [5]. However, the reason for this discrepancy was not clear to previous investigators. Kotsovinos [8] and Kotsovinos and List [9] pointed out that due to the non-linear relation between water density and temperature (or non-constant thermal expansion coefficient of the water), the thermal buoyancy flux is not conserved, but it is the heat flux which is conserved. They showed that the buoyancy flux at some distance from the exit was reduced to 50% of its initial value. Kotsovinos [8] presented a numerical model for the vertical buoyant jet considering variable thermal buoyancy flux.

Therefore we require in this numerical model the conservation of heat flux instead of the conservation of the buoyancy flux. The buoyancy at each cross-section is calculated from the integral of the density profile across the jet, where the density profile is calculated from the temperature profile using an accurate non-linear relationship between density and temperature, for example:

$$\bar{\rho} = 1 + ((A_0 + A_1 \bar{T}_m + A_2 \bar{T}_m^2 + A_3 \bar{T}_m^3)/1000), \tag{13}$$

where $A_0 = -0.09462134700$, $A_1 = 0.0513121236000$, $A_2 = -0.00738763631$, $A_3 = 0.0000326214688$.

2.3. The coefficient of entrainment, α_e defined as

$$\frac{d}{ds} \int_{-B(s)}^{+B(s)} \bar{u}(s,n) dn = 2\alpha_e \bar{u}_m$$

is a function of the local Richardson (or local Froude) number and according to Kotsovinos [8] is given by the equation

$$2\alpha_e \bar{u}_m = (q_0 + q_1 R_{ch}) \frac{m}{\mu}, \tag{14}$$

where q_0 and q_1 are experimental constants which for vertical plane buoyant jets obtain the values $q_0 = 0.146$ and $q_1 = 0.252$. The same values are adopted in this numerical model. The maximum value of α_e used in this work was 0.11, even though the obtaining from Eq. (14) was greater.

To simplify the problem the usual approach is to integrate the above set of equations across the buoyant jet assuming that the time averaged mean velocity profile normal to the jet axis, the time-averaged mean temperature profile and time-averaged mean density profile are given by the Gaussians:

$$\bar{u}(s,n) = \bar{u}_m \exp(-n^2/b_{1/eu}^2), \tag{15}$$

$$\frac{\rho_a - \bar{\rho}(s,n)}{\rho_a} = \frac{\rho_a - \bar{\rho}_m}{\rho_a} \exp(-n^2/(\lambda b_{1/eu})^2), \tag{16}$$

$$\bar{T}(s,n) = \bar{T}_m \exp(-n^2/(\lambda b_{1/eu})^2), \tag{17}$$

where $\bar{u}_m$, $\bar{\rho}_m$, $\bar{T}_m$ are the mean values of the velocity, density and temperature at jet axis, $b_{1/eu}$ is the value of n at which the mean velocity takes the value $\bar{u}_m/e$, $b_{1/eT}$ is the value of n at which the mean temperature takes the value $\bar{T}_m/e$, λ is the ratio of these two widths i.e. $\lambda = b_{1/eT}/b_{1/eu}$. Typical value for λ for the vertical buoyant jet is 1.2–1.3, see Kotsovinos [8], List [2]. Furthermore, we make the following assumption and approximation: the pressure is everywhere hydrostatic. This assumption simplifies the model, but is not correct (see Kotsouinos and Angelidis [13]) and for a jet out of a wall of significant. In our case it estimated that this error is of the order of ±2%.

The integrated across the jet equations give therefore the following set of equations (see also Fig. 1 for the symbols):

Continuity:

$$\frac{d}{ds}[\bar{u}_m b_{1/eu}] = 2\alpha_e \bar{u}_m/\sqrt{\pi}. \tag{18}$$

x-momentum:

$$\frac{d}{ds}\left[\frac{\bar{u}_m^2 b_{1/eu}}{\sqrt{2}}\cos\theta\right] = 0. \tag{19}$$

y-momentum:

$$\frac{d}{ds}\left[\frac{\bar{u}_m^2 b_{1/eu}}{\sqrt{2}}\sin\theta\right] = g\lambda b_{1/eu}\frac{\rho_a - \bar{\rho}_m}{\rho_a}. \tag{20}$$

Heat flux:

$$\begin{aligned} H_0 &= \rho c_p \int_{-B(s)}^{+B(s)} \bar{u}(s,n)\bar{T}(s,n)\,dn + \int_{-B(s)}^{+B(s)} \overline{u'T'}\,dn \\ &= H_M + H_T = H_M + (0.06 + 0.51R_{ch}(s))H_0, \end{aligned} \tag{21}$$

where c_p is the specific heat of water. Combining the above equations, we find the following set of seven linear differential equations:

$$\frac{dx}{ds} = \cos\theta, \tag{22}$$

$$\frac{dy}{ds} = \sin\theta, \tag{23}$$

$$\frac{d\theta}{ds} = \frac{\sqrt{2}g\lambda}{\bar{u}_m^2}\frac{\rho_a - \bar{\rho}_m}{\rho_a}\cos\theta, \tag{24}$$

$$\begin{aligned} \frac{d(\bar{T}_m - T_a)}{ds} = &-\frac{2\alpha_e}{\sqrt{\pi}b_{1/eu}}(\bar{T}_m - T_a) \\ &+ \left[\frac{\omega}{\bar{\rho}_m\bar{u}_m^3} - \frac{\left(\bar{T}_m - T_a\right)}{\bar{\rho}_m}\right]\left(\frac{d\bar{\rho}_m}{ds}\right) \\ &- \omega\frac{\rho_a - \bar{\rho}_m}{\bar{\rho}_m\bar{u}_m^3 b_{1/eu}}\left(\frac{db_{1/eu}}{ds}\right) \\ &+ \frac{2\omega(\rho_a - \bar{\rho}_m)}{\bar{\rho}_m\bar{u}_m^4}\left(\frac{d\bar{u}_m}{ds}\right), \end{aligned} \tag{25}$$

where $\omega = 1.442\rho_0 u_0 T_0 Dg/\rho_a$,

$$\frac{d\bar{u}_m}{ds} = \frac{\sqrt{2}g\lambda}{\bar{u}_m}\frac{\rho_a - \bar{\rho}_m}{\rho_a}\sin\theta - \frac{2\alpha_e\bar{u}_m}{\sqrt{\pi}b_{1/eu}}, \tag{26}$$

$$\frac{db_{1/eu}}{ds} = \frac{4\alpha_e}{\sqrt{\pi}} - \frac{\sqrt{2}g\lambda b_{1/eu}}{\bar{u}_m^2}\frac{\rho_a - \bar{\rho}_m}{\rho_a}\sin\theta, \tag{27}$$

$$\frac{d\bar{\rho}_m}{ds} = \left(A_1\frac{1}{1000} + A_2\frac{2}{1000}\bar{T}_m + A_3\frac{3}{1000}\bar{T}_m^2\right)\left(\frac{d\bar{T}_m}{ds}\right), \tag{28}$$

where

$$\alpha_e = 0.0550 + 0.089\sqrt{\frac{8\pi\lambda^2}{(1+\lambda^2)\ln 2}}\frac{1}{F_L^2} \tag{29}$$

and

$$F_L = \frac{\bar{u}_m}{\sqrt{g\frac{\rho_a - \bar{\rho}_m}{\rho_a}b_u}}. \tag{30}$$

In the above system of ordinary differential equations (22)–(28) there are seven unknowns i.e. x, y, θ, $\bar{T}_m$, $\bar{u}_m$, $b_{1/eu}$, $\bar{\rho}_m$ which are, respectively, the coordinates x and y of the jet axis, the angle of inclination, the mean axial temperature, the mean axial velocity, the width of the velocity profile of the jet, and the axial mean density.

The numerical model starts the integration at the end of flow establishment which occurs at a distance equal to $6D$ (where D is the width of the plane jet at the exit). The boundary conditions are the initial values for the unknown parameters

$$x, y, \theta, \bar{T}_m, \bar{u}_m, b_{1/eu}, \bar{\rho}_m$$

calculated at the end of flow establishment. Specifically it is assumed at $s = 0$,

$$x = 6D, \tag{31}$$

$$y = 0, \tag{32}$$

$$\theta = 0, \tag{33}$$

$$\bar{T}_m(s=0) = 0.73(T_0 - T_a) + T_a, \tag{34}$$

$$\bar{u}_m(s=0) = 0.82U_0, \tag{35}$$

$$b_{1/eu}(s=0) = \sqrt{2/\pi}D, \tag{36}$$

$$\begin{aligned} &\bar{\rho}_m(s=0) \\ &\quad = 1 + ((A_0 + A_1\bar{T}_m + A_2\bar{T}_m^2 + A_3\bar{T}_m^3)/1000). \end{aligned} \tag{37}$$

The solution is found using the variable order Adams predictor corrector method. The numerical solution is compared subsequently with experimental results.

3. Experimental procedure

In this work, a heated plane buoyant jet was produced by discharging horizontally hot water from 84 round ports of a diffuser of diameter 10 cm. The diameter of the ports was 0.305 cm, their spacing was 0.70 cm, and the length of the diffuser was 58.4 cm. The individual jets from the multiport diffuser merged at a distance about 1 cm from their exit, forming a plane buoyant jet. The equivalent width of the slit of the plane buoyant jet is 0.105 cm. The buoyant jet discharged into a tank 4.5×2.7 and 2 m deep with glass walls filled with water of uniform temperature. The horizontal buoyant jet was confined by two Plexiglas walls 59 cm apart in order to maintain two dimensionality of the flow. The multiport diffuser and the confining Plexiglas walls were positioned 38.5 cm above the tank bottom to permit freely the entrainment of ambient water. A constant head tank supplied the jet through a calibrated flowmeter. In all the experiments the tracer concentration measured was the excess temperature of the jet fluid above the ambient fluid. A sketch of the experimental apparatus is given in Fig. 2.

Instantaneous temperature measurements from a rank of 30 thermistors, mounted on a stainless steel tube to form a probe positioned either horizontally or vertically, were recorded for 120 s at a sampling frequency of 40 samples/s.

The measurements were taken using ultra-fast response thermistors (time constant 7 ms) of bead diameter 0.125 mm and the dissipation constant in still water at 25 °C was 0.25 mV/°C. The shelf-heating of the thermistor due to Ohmic dissipation was less than 0.006 °C.

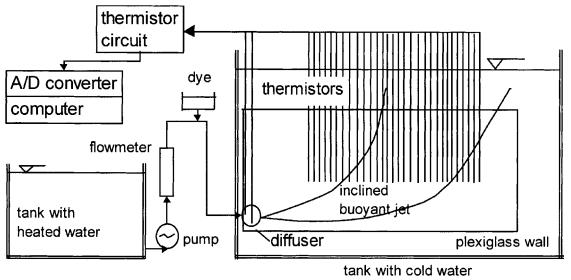

Fig. 2. A sketch of the experimental apparatus.

The thermistors were calibrated at the beginning of an experiment to minimize the drift and ageing problems. The thermistors temperature response was measured with a bridge circuit, and the instantaneous analog voltages were recorded using a data acquisition system and a PC. Each thermistor was individually calibrated and a third-order polynomial fitted to the set of calibration points in the least-squares sense. The used thermistors were made by the company "THERMOMETRICS INC" (USA) and belong to the FP07 series.

4. Comparison of the numerical model with experimental results

A substantial number of experiments on plane buoyant jets were performed using the apparatus and techniques described in the previous section. In these experiments, mean temperature and turbulence intensity profiles were measured for jets with different initial

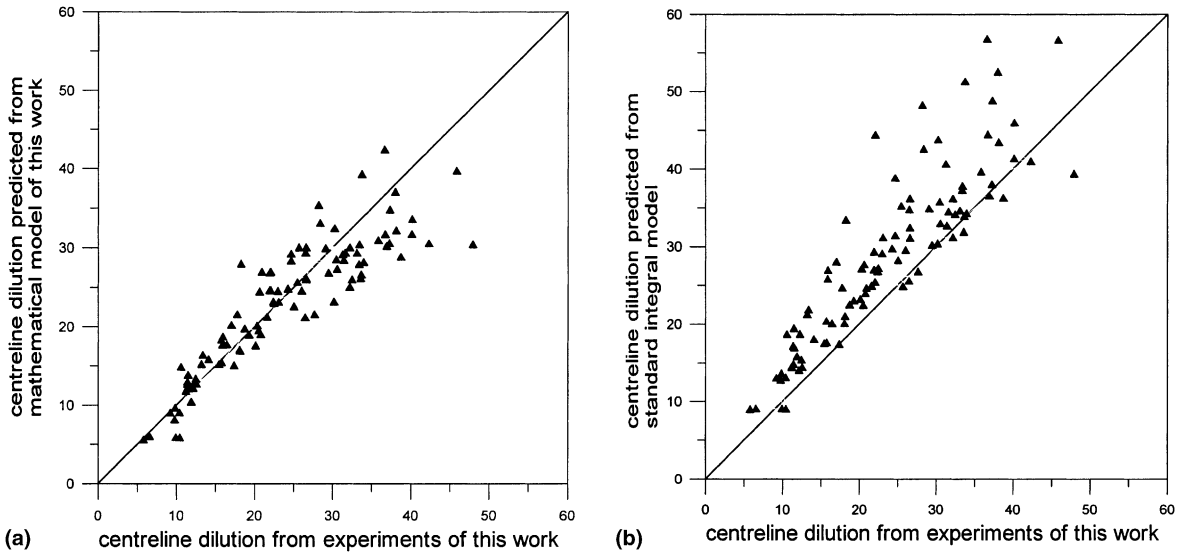

Fig. 3. Comparison of the centerline dilution determined experimentally from temperature profiles of this work with: (a) the prediction of the mathematical model of this work; (b) the prediction of the standard integral model.

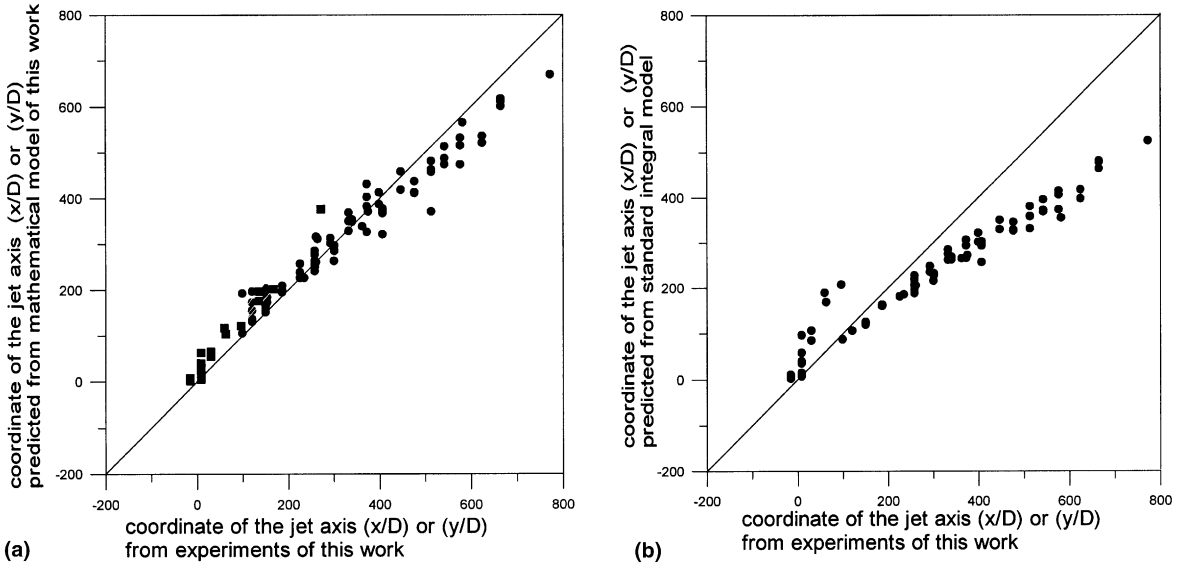

Fig. 4. Comparison of the coordinate of the jet axis determined experimentally from temperature profiles of this work with: (a) the prediction of the mathematical model of this work; (b) the prediction of the standard integral model.

Froude numbers. A total of 99 temperature cross-sections were measured. The initial Froude numbers F_0 varied from 11.5 to 72.0.

The experimental results of this study for the axial dilution are compared with the numerical prediction in Fig. 3. These experimental results are compared in Fig. 3(a) with predictions from the improved mathematical model of this work. The same experimental results are compared in Fig. 3(b) with predictions from the standard integral model of the type that Fan and Brooks [3] used. As we see the improved mathematical model of this work predicts reasonably well the centerline dilution determined experimentally from 99 temperature profiles and its prediction is generally better than the prediction of the standard integral model.

Comparison with the numerical prediction of the location of the buoyant jet axis, determined experimentally from 99 temperature profiles is shown in Fig. 4. Coordinates x/D or y/D of the axis are plotted, because the corresponding y/D or x/D coordinates are known from the probes' places, which positioned either horizontally or vertically. The experimental results for the location of the buoyant jet axis are compared in Fig. 4(a) with predictions from the improved mathematical model of this work. The same experimental results are compared in Fig. 4(b) with predictions from the standard integral model. It is observed that the numerical model of this work predicts reasonably well the location of the jet axis and its prediction is generally better than the prediction of the standard integral model.

A comparison is given in Fig. 5 of the location of the jet axis determined experimentally from the temperature profiles with the prediction of the improved mathematical model of this work and with the prediction of the standard integral model. In all cases, the mathematical model of this work predicts in a more accurate way the jet axis.

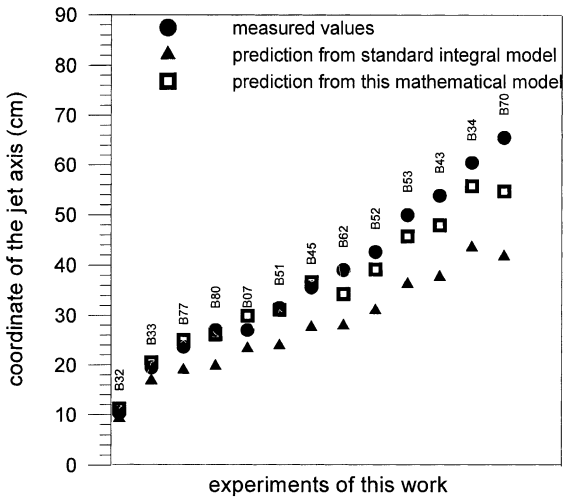

Fig. 5. Comparison of the coordinate of the jet axis determined experimentally from temperature profiles with the prediction of the mathematical model of this work and with the prediction of the standard integral model.

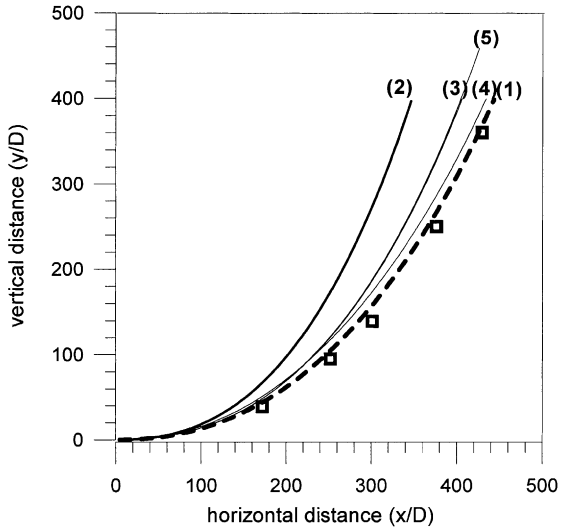

Fig. 6. Comparison of the jet axis determined experimentally (noted as □) with the prediction of the following mathematical models: (1) mathematical model of this work; (2) standard integral model; (3) mathematical model of this work without the contribution of turbulent heat flux; (4) mathematical model of this work with constant entrainment coefficient; (5) mathematical model of this work using conservation of buoyancy flux instead of heat flux.

The experimental results for the location of the jet axis – noted with the symbol □ – and the trajectory predicted from the improved mathematical model of this work, which named as (1), are drawn in Fig. 6. Also the trajectory predicted from the standard integral model is drawn and named as (2). The trajectory named as (3) is a result of neglecting the contribution of the turbulent heat flux from the mathematical model of this work. The trajectory named as (4) comes from the mathematical model of this work using however constant entrainment coefficient. The trajectory named as (5) comes from the mathematical model of this work using conservation of buoyancy flux instead of heat flux. It is also observed the influence of the inclusion of the turbulent heat flux, the effect of using constant entrainment coefficient and

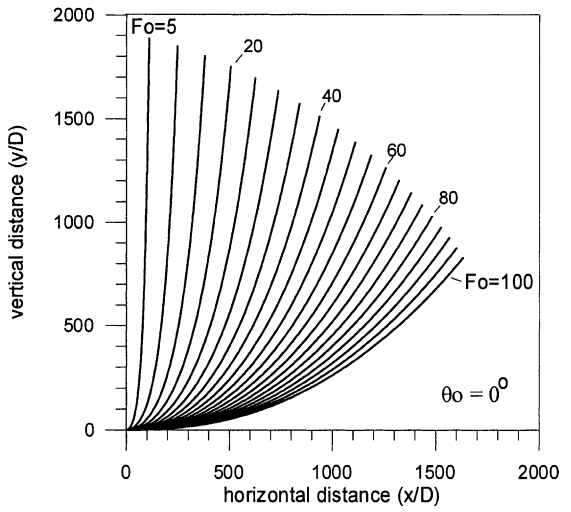

Fig. 7. Trajectories for various Froude numbers as they predicted from the numerical model for the horizontal buoyant jet.

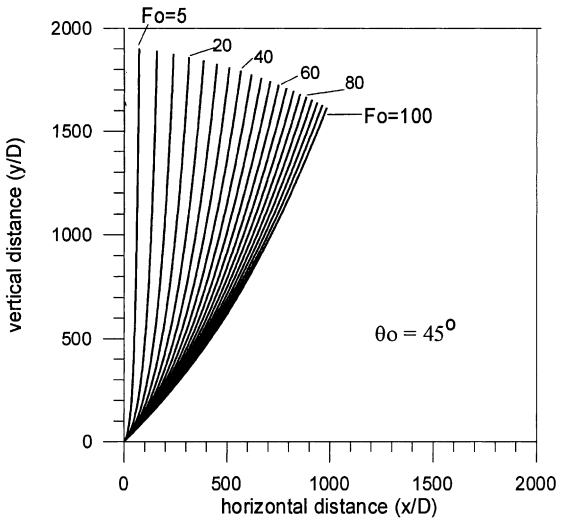

Fig. 8. Trajectories for various Froude numbers as they predicted from the numerical model for an inclined ($\theta_0 = 45°$) buoyant jet.

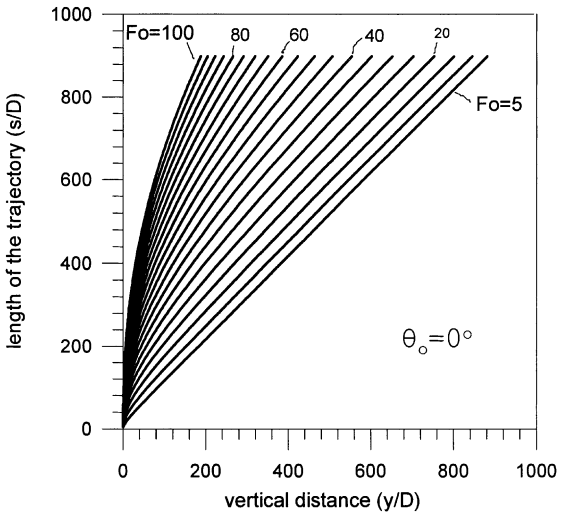

Fig. 9. Normalized length of the trajectory of a horizontal buoyant jet as a function of the normalized vertical distance for various initial Froude numbers F_0.

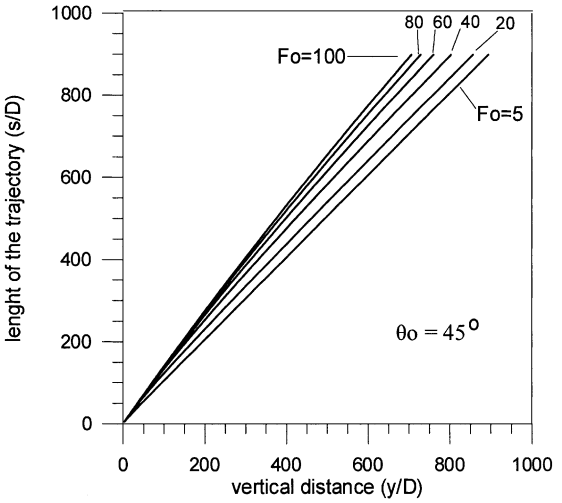

Fig. 10. Normalized length of the trajectory of an inclined buoyant jet ($\theta_0 = 45°$) as a function of the normalized vertical distance for various initial Froude numbers F_0.

the effect of using conservation of buoyancy flux instead of heat flux too. It is observed that the mathematical model of this work really improves the standard integral model.

Trajectories for various initial Froude numbers (from 5 to 100) are plotted in Figs. 7 and 8, as they predicted from the numerical model. The initial angle of the inclination θ_0 is equal to 0° in Fig. 7, which corresponds to the horizontal submerged heated plane buoyant jet. In Fig. 8, the initial angle of inclination θ_0 is equal to 45°.

Table 1
Polynomial coefficients for calculation of the normalized length of the trajectory (s/D) of a horizontal buoyant jet as a function of the normalized vertical distance (y/D) for various initial Froude numbers F_0

F_0	$(s/D) = a + b(y/D) + c(y/D)^2$		
	a	b	c
5	13.1952	1.01652	−1.41687E − 05
10	31.3543	1.08456	−7.43328E − 05
15	47.0401	1.19428	−1.77202E − 04
20	60.3192	1.33815	−3.23013E − 04
30	81.1829	1.71564	−7.66952E − 04
40	96.3368	2.21102	−1.48996E − 03
50	107.2730	2.83298	−2.63188E − 03
60	115.0560	3.59138	−4.38533E − 03
70	120.5360	4.49568	−7.00201E − 03
80	124.3680	5.55122	−1.07852E − 02
90	127.0450	6.76334	−1.61021E − 02
100	128.9390	8.13079	−2.33519E − 02

Table 2
Polynomial coefficients for calculation of the normalized length of the trajectory (s/D) of an inclined buoyant jet ($\theta_0 = 45°$) as a function of the normalized vertical distance (y/D) for various initial Froude numbers F_0

F_0	$(s/D) = a + b(y/D) + c(y/D)^2$		
	a	b	c
5	4.3751	1.00170	0.00000E + 00
20	11.1863	1.09683	−7.42373E − 05
40	9.3777	1.23234	−1.62184E − 04
60	5.5487	1.32309	−2.00425E − 04
80	2.8483	1.37348	−2.01038E − 04
100	1.3016	1.39933	−1.83645E − 04

Usually engineers design diffusers according to the centerline concentration and they use semi-empirical formulas for this scope. The necessary parameter which must be calculated is the length of the trajectory s. We present subsequently diagrams and polynomial equations to help design engineers.

The normalized length of the trajectory (s/D) as a function of the normalized vertical distance (y/D) for various initial Froude numbers F_0 is plotted in Figs. 9 and 10. The angle $\theta_0 = 0°$ (Fig. 9) corresponds to the horizontal buoyant jet and the angle $\theta_0 = 45°$ (Fig. 10) corresponds to the inclined buoyant jet. We have applied a polynomial curve fitting of second degree to these data. The calculated polynomial coefficients for various Froude numbers F_0 are given in Tables 1 and 2 for the horizontal ($\theta_0 = 0°$) and the inclined ($\theta_0 = 45°$) cases. These polynomial functions are valid for $50 < s/D < 800$.

5. Conclusion–discussion

The mathematical model of this study for the mixing of an inclined submerged heated plane water jet has three significant improvements over similar previous models: (a) the conservation of heat flux instead of the conservation of the buoyancy flux, (b) the inclusion of the turbulent heat flux integrated across the jet, and (c) the modification to use an entrainment function that varies with Richardson number. The agreement of the numerical model with the experimental results of this study for the axial dilution and the trajectory indicates reasonable accuracy (see Figs. 3–6). The inclusion of the turbulent heat flux and the conservation of buoyancy flux instead of heat flux in the numerical model improve the overall accuracy of the model. In all cases, the mathematical model of this work predicts in a more accurate way the axial dilution and the jet trajectory than the standard integral model. The length of the trajectory s resulting easily from diagrams or from simple polynomial functions is useful for engineers to design diffusers.

References

[1] E.J. List, Turbulent jets and plumes, Ann. Rev. Fluid Mech. 14 (1982) 189–212.
[2] E.J. List, in: W. Rodi (Ed.), Turbulent buoyant jets and plumes, Pergamon, Oxford, 1982, pp. 1–68 (Chapter 1).
[3] L.N. Fan and N.H. Brooks, Numerical solutions of turbulent buoyant jet problems, KH-R-18W, M. Keck Laboratory of Hydraulics and Water Resources, California Institute of Technology, 1969.
[4] H. Anwar, Behavior of buoyant jet in calm fluid, J. Hydraul. Div. 95 (1969).
[5] T.L. Chan, J.F. Kennedy, Submerged buoyant jets in quiescent fluids, J. Hyd. Div., ASCE 101 (1975) 733–747.
[6] J.H.W. Lee, Generalized lagrangian model for buoyant jets in current, J. Environ. Eng. 116 (1990) 1085–1106.
[7] E.A. Hirst, Buoyant jets with three-dimensional trajectories, J. Hyd. Div., ASCE 98 (1971) 1999–2014.
[8] N.E. Kotsovinos, A study of the entrainment and turbulence in a plane buoyant jet, Ph.D. Thesis, California Institute of Technology, Pasadena, 1975.
[9] N.E. Kotsovinos, E.J. List, Plane turbulent buoyant jets. Part. 1 Integral properties, J. Fluid Mech. 81 (1977) 25–44.
[10] P.B. Angelidis, Modeling of pollution from two dimensional horizontal buoyant jet, Ph.D. Thesis, Democtitus University of Thrace, Xanthi, Greece, 1993.
[11] B. Morton, G.I. Taylor, J.S. Turner, Turbulent gravitational convection from maintained and instantaneous sources, Proc. Royal Soc. A (1956) 1–23.
[12] G.P. Lemieux, An experimental study of the effects of Reynolds number and buoyancy upon the structure of inclined turbulent two-dimensional jets, Ph.D. Thesis, Queen's University, Kingston, Ont., 1983.
[13] N.E. Kotsovinos, P.B. Angelidis, The momentum flux in turbulent submerged jets, J. Fluid Mech. 229 (1991) 453–470.